Hindawi Publishing Corporation
Journal of Control Science and Engineering
Volume 2015, Article ID 604257, 15 pages
http://dx.doi.org/10.1155/2015/604257

Research Article

LMI Based Fuzzy Control of a Wing Doubled Fractional-Order Chaos

Bin Wang, Yuzhu Wang, Hongbo Cao, and Delan Zhu

Department of Electrical Engineering, Northwest A&F University, Yangling 712100, China

Correspondence should be addressed to Delan Zhu; dlzhu@126.com

Received 26 January 2015; Revised 9 June 2015; Accepted 10 June 2015

Academic Editor: Hung-Yuan Chung

This paper investigates a new wing doubled fractional-order chaos and its control. Firstly, a new fractional-order chaos is proposed, replacing linear term x in the second equation by its absolute value; a new improved system is got, which can make the wing of the original system doubled. Then, circuit diagram is presented for the proposed fractional-order chaos. Furthermore, based on fractional-order stability theory and T-S fuzzy model, a more practical stability condition for fuzzy control of the proposed fractional-order chaos is given as s set of linear matrix inequality (LMI) and the strict mathematical norms of LMI are presented. Finally, numerical simulations are given to verify the effectiveness of the proposed theoretical results.

1. Introduction

Fractional calculus has the same history as integer calculus, which has appeared 300 years ago. Nevertheless, it has not been widely used in actual project until recent decades [1–4]. Recently, people find that many actual systems can be well described with the help of fractional calculus, especially for memory and hereditary properties of various materials and processes [5–7]. For example, it can be better described with fractional calculus of power system [8], memristor system [9], physical system [10], chemical system [11], and so on.

It has been widely verified that chaos is universal in integer-order chaos. For the advantages of fractional-order chaotic systems in secure communication and signal processing [12–14], many new fractional-order chaotic systems have been proposed and analyzed. For example, Chen et al. proposed a new fractional-order chaotic system and the circuit synchronization of the system was implemented which was very important in theory and practice [15]. Jia et al. studied the chaotic features of the fractional-order Lorenz system and the circuit implementation was presented [16]. A new fractional-order hyperchaotic system based on the Lorenz system was presented and the fractional Hopf bifurcation was investigated in [17]. A new three-dimensional King Cobra face shaped fractional-order chaotic system was designed and the multiscale synchronization of two identical fractional-order King Cobra chaotic systems was derived through feedback control in [18]. In particular, since the potential merits of fractional-order chaos in secure communication and many other fields, fractional-order chaos control and synchronization has become a hot topic.

Many studies indicated that integer-order chaos could be well controlled. Recently, many scholars tried to investigate the control methods for fractional-order chaotic systems. Until now, some control strategies have been designed for the control of fractional-order chaotic systems such as sliding mode control [19], finite time control [20], and pinning control [21], among many others. Fuzzy control is well known as an effective control strategy, and it has attracted more and more scholar's attention. Linear matrix inequality (LMI), as a very important and classic tool, has been widely used in the fuzzy control and synchronization of integer-order chaos. For example, in [22], by employing LMI method, a new fuzzy controller based on T-S fuzzy model is designed for chaos synchronization of two Rikitake generator systems. In [23], a T-S fuzzy receding horizon H-infinity synchronization (TSFRHHS) approach is proposed and a novel set of LMI conditions are given. And the scheme is applied to synchronize Lorenz meteorological chaos. In [24], a robust static output feedback controller is derived in strict LMI terms for discrete-time T-S fuzzy systems. However, this control method has been mostly used in integer-order systems up to now. As we all know, the controllability and stability region of fractional-order systems are different with integer-order systems. Can LMI be applied to the fuzzy control of the wing doubled fractional-order chaos? If so, what are the special application conditions and strict mathematical norms? There is almost no relevant literature. Research in this area should be meaningful and challenging.

In light of the above analysis, there are three advantages which make our research attractive. Firstly, a new wing doubled fractional-order chaos is proposed and its experimental circuit simulation is presented. Secondly, based on fractional-order stability theory, a more practical stability condition for fuzzy control of the proposed fractional-order chaos is proposed and the strict mathematical norms of LMI are presented. Finally, numerical simulations are given to verify the effectiveness of the proposed theoretical results.

The paper is organized as follows. In Section 2, the fractional-order calculus and stability theory are presented. Section 3 introduces the system description and circuit implementation. In Section 4, the fuzzy controller design and numerical simulations are presented. Conclusions are drawn in Section 5.

2. Preliminaries

2.1. Fractional-Order Calculus. There are two commonly used definitions of fractional calculus operator: Riemann-Liouville definition and Caputo definition, which are listed here for clarity.

Definition 1. The Riemann-Liouville fractional integral is described as

$$J_{t0}^{q} f(x) = \frac{1}{\Gamma(q)} \int_{t0}^{t} (t-\tau)^{q-1} f(\tau)\, d\tau, \tag{1}$$

where $q \in R^{+}$, $f : R \rightarrow R$, J_{t0}^{q} denotes q order integral operator, $\Gamma(\cdot)$ means the Gamma function, and $\Gamma(q) = \int_{0}^{\infty} t^{q-1} e^{-t} dt$.

Definition 2. The Riemann-Liouville fractional derivative is given by

$$\begin{aligned} D_{t0}^{q} f(t) &= D_{t0}^{n} J_{t0}^{n-q} f(t) \\ &= \begin{cases} \dfrac{d^n}{dt^n}\left[\dfrac{1}{\Gamma(n-q)} \displaystyle\int_{t0}^{t} (t-\tau) f(\tau)\, d\tau\right], & n-1 < q < n, \\ \dfrac{d^n}{dt^n} f(t), & q = n, \end{cases} \end{aligned} \tag{2}$$

where D_{t0}^{q} denotes q order Riemann-Liouville derivative operator.

Definition 3. The Caputo derivative can be written by

$$\begin{aligned} {}_{0}^{c}D_{t0}^{q} f(t) &= J_{t0}^{n-q} D_{t0}^{n} f(t) \\ &= \begin{cases} \dfrac{1}{\Gamma(n-q)} \displaystyle\int_{t0}^{t} (t-\tau)^{n-q-1} f^{(n)}(\tau)\, d\tau, & n-1 < q < n, \\ \dfrac{d^n}{dt^n} f(t), & q = n, \end{cases} \end{aligned} \tag{3}$$

where ${}_{0}^{c}D_{t0}^{q}$ denotes q order Caputo derivative operator, which can be simplified as D^{q}.

The Caputo derivative has a popular application in engineering and is adopted in this paper.

2.2. Stability in Fractional-Order Systems

Theorem 4 (see [25]). *Consider the following linear fractional-order system:*

$$D^{q} x = Ax, \quad x(0) = x_0, \tag{4}$$

where $A \in R^{n\times n}$, $x \in R^{n}$, and $q = [q_1, q_2, \ldots, q_i, \ldots, q_n]$ $(0 < q_i \leq 1)$. System (4) is asymptotically stable if and only if $|\arg(\lambda_i)| > q\pi/2$ is satisfied for all eigenvalues λ_i of matrix A. Besides, this system is stable if and only if $|\arg(\lambda_i)| \geq q\pi/2$ is satisfied for all eigenvalues λ_i of matrix A and those critical eigenvalues, which satisfy condition $|\arg(\lambda_i)| = q\pi/2$, have geometric multiplicity one.

3. New Wing Doubled System and Circuit Simulation

3.1. System Model. A new three-dimensional fractional-order chaos is written as

$$\begin{aligned} \frac{d^q x}{dt^q} &= \frac{28}{11} x - yz, \\ \frac{d^q y}{dt^q} &= -10y + xz + kx, \\ \frac{d^q z}{dt^q} &= -4z + xy, \end{aligned} \tag{5}$$

where x, y, and z are the state variables, k is a real number, here, $k = 0.2$, and q is the fractional-order. In order to study the chaotic characteristics of system (5), firstly, it is easy to get the Jacobian matrix:

$$\begin{aligned} \lambda_1 &= -10.0000, \\ \lambda_2 &= 2.5455, \\ \lambda_3 &= -4.0000 \\ J_0 &= \begin{bmatrix} \dfrac{28}{11} & -z & -y \\ z+0.2 & -10 & x \\ y & x & -4 \end{bmatrix}. \end{aligned} \tag{6}$$

Table 1

Equilibrium points	Their corresponding eigenvalues
$E_1(0, 0, 0)$	$\lambda_1 = -10.0000, \lambda_2 = 2.5455, \lambda_3 = -4.0000$
$E_2(-6.4512, 3.1909, -5.1462)$	$\lambda_1 = 1.1552 + 5.3713i, \lambda_2 = 1.1552 - 5.3713i, \lambda_3 = -13.7650$
$E_3(-6.2004, -3.1909, -4.9462)$	$\lambda_1 = -11.4914, \lambda_2 = 0.0368, \lambda_3 = 0$
$E_4(6.2004, 3.1909, 4.9462)$	$\lambda_1 = 1.0344 + 5.3349i, \lambda_2 = 1.0344 - 5.3349i, \lambda_3 = -13.5233$
$E_5(6.4512, -3.1909, -5.1462)$	$\lambda_1 = 1.1552 + 5.3713i, \lambda_2 = 1.1552 - 5.3713i, \lambda_3 = -13.7650$

Besides, the dynamic characteristics of the system are related to the eigenvalues. Eigenvalues are determined by the Jacobian matrix at equilibrium points. System (5) has five equilibrium points; the corresponding eigenvalues are given as in Table 1.

According to Theorem 4, nonstable region is determined by the following conditions:

$$\begin{aligned} q\frac{\pi}{2} &\geq \min_i \{\arg|\lambda_i|\} = \max_i \left\{\arctan \frac{|\mathrm{Im}(\lambda_i)|}{|\mathrm{Re}(\lambda_i)|}\right\} \\ &= \arctan \frac{5.3349}{1.0344} = 1.3793 \\ &\longrightarrow q > 0.8781. \end{aligned} \tag{7}$$

Therefore, the necessary conditions for generating chaos of system (5) is $q > 0.8781$, and this paper takes $q = 0.9$. The phase trajectories of system (5) are shown in Figure 1 with the initial value $(x(0), y(0), z(0)) = (20, 0.6, 0.8)$. We can clearly see that the system has two-wing chaotic attractor.

Now we replace the linear term x in the second equation of system (5) by its absolute value $|x|$; a new improved system can be got:

$$\begin{aligned} \frac{d^q x}{dt^q} &= \frac{28}{11}x - yz, \\ \frac{d^q y}{dt^q} &= -10y + xz + k|x|, \\ \frac{d^q z}{dt^q} &= -4z + xy. \end{aligned} \tag{8}$$

Note that system (8) has certain symmetry. Removing the absolute value of the second equation, each equation contains the corresponding linear term and the cross product term of the other two state variables. Figure 2 shows the phase trajectories of system (8) when $k = 0.2$; in this case, we can see that system (8) has four-wing structure and four chaotic attractors, which realize the wing doubled system (5).

3.2. Circuit Simulation. Fractional circuit is generally expressed as follows:

$$F(s) = \frac{R_1}{sR_1C_1 + 1} + \frac{R_2}{sR_2C_2 + 1} + \cdots \frac{R_n}{sR_nC_n + 1}, \tag{9}$$

where n is the unit number of basic integration circuit.

According to the literature [26], when the fractional-order is 0.9, (9) can be written as

$$F(s) = \frac{R_1}{sR_1C_1 + 1} + \frac{R_2}{sR_2C_2 + 1} + \frac{R_3}{sR_3C_3 + 1}, \tag{10}$$

where $R_1 = 62.84\,\mathrm{M\Omega}$, $R_2 = 250\,\mathrm{k\Omega}$, $R_3 = 2.5\,\mathrm{k\Omega}$, $C_1 = 1.232\,\mu\mathrm{F}$, $C_2 = 1.835\,\mu\mathrm{F}$, and $C_3 = 1.1\,\mu\mathrm{F}$. The unit circuit of (10) is shown in Figure 3.

System (5) is rewritten as the following corresponding circuit equation:

$$\begin{aligned} \frac{d^{0.9}x}{dt^{0.9}} &= \frac{R_3}{R_2R_4C_0}x - \frac{R_3}{R_1R_4C_0}yz \\ \frac{d^{0.9}y}{dt^{0.9}} &= -\frac{R_7}{R_8}\frac{R_5}{R_{15}R_6C_0}y + \frac{R_5}{R_{14}R_6C_0}xz + \frac{R_5}{R_{14}R_6C_0}x \\ \frac{d^{0.9}z}{dt^{0.9}} &= -\frac{R_{11}}{R_{18}}\frac{R_9}{R_{17}R_{10}C_0}z + \frac{R_9}{R_{16}R_{10}C_0}xy. \end{aligned} \tag{11}$$

The designed overall circuit diagram is shown in Figure 4. Each channel of the circuit is formed by resistors, capacitors, operational amplifiers, and multiplier. There are three channels, representing the three states of system (5). The circuit parameters of system (5) are designed as follows: $R_1 = 700\,\mathrm{k\Omega}$, $R_2 = 275\,\mathrm{k\Omega}$, $R_3 = 14\,\mathrm{k\Omega}$, $R_4 = R_6 = 20\,\mathrm{k\Omega}$, $R_5 = 7\,\mathrm{k\Omega}$, $R_{10} = 25\,\mathrm{k\Omega}$, $R_7 = R_8 = R_{11} = R_{17} = R_{18} = 10\,\mathrm{k\Omega}$, $R_{13} = 700\,\mathrm{k\Omega}$, $R_{14} = 350\,\mathrm{k\Omega}$, $R_{15} = 35\,\mathrm{k\Omega}$, and $R_{16} = 40\,\mathrm{k\Omega}$; C_0 is the unit circuit of Figure 3.

Figure 5 shows the simulation results of the fractional-order system (5); we can see that the circuit simulation results in Figures 5(a)–5(c) are in line with the phase diagram in Figures 1(a)–1(c). It indicates that the proposed fractional-order system (5) can be realized by circuit simulation, and the circuit diagram is valid and practical.

Similarly, the designed circuit diagram of system (8) is shown in Figure 6, and the corresponding simulation results are presented in Figure 7. We can also see that the circuit simulation results in Figures 7(a)–7(c) are in line with the phase diagram in Figures 2(a)–2(c). It indicates that the wing doubled system (8) can be easily achieved by circuit simulation. Therefore, the circuit diagram of system (8) is valid and practical.

4. Controller Design and Numerical Simulations

4.1. T-S Fuzzy Model. The fractional-order T-S fuzzy model is given in the following form:

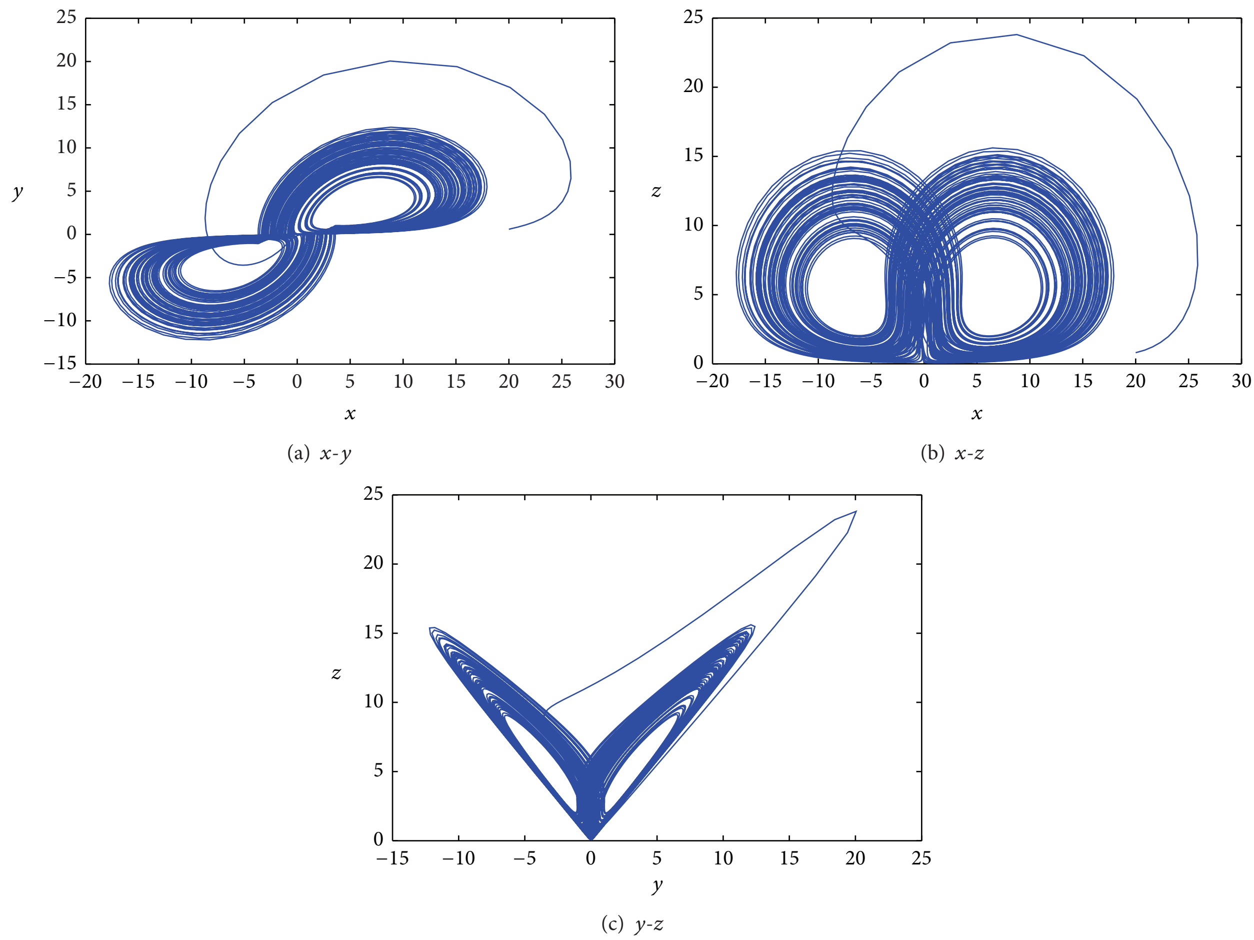

Figure 1: Phase trajectories of fractional-order chaotic system (5).

Rule R^i is as follows: IF $z_1(t)$ is M_{i1} and $\cdots$ and $z_n(t)$ is M_{in}

$$\text{THEN } \frac{d^q x}{dt^q} = A_i x(t) + B_i u(t) \quad (i = 1, 2, \ldots, r), \tag{12}$$

where M_{ij} $(j = 1, 2, \ldots, r)$ is the fuzzy set and r is the number of IF-THEN rules, $x(t) \in R^n$ is the state vector, $A_i \in R^{n\times n}$, $z(t) = [z_1(t), z_2(t), \ldots, z_n(t)]$ are the premise variables, and q is the fractional-order; $u(t)$ is control input.

By adopting single point fuzzification, product inference, and weighted average defuzzification, the final output of the fractional-order T-S fuzzy model is inferred as follows:

$$\frac{d^q x}{dt^q} = \sum_{i=1}^{r} h_i(z(t)) A_i x(t) + \sum_{i=1}^{r} h_i(z(t)) B_i u(t), \tag{13}$$

where

$$h_i(z(t)) = \frac{\prod_{j=1}^{n} M_{ij}(z_j(t))}{\sum_{i=1}^{r} \prod_{j=1}^{n} M_{ij}(z_j(t))} \geq 0, \qquad \sum_{i=1}^{r} h_i(z(t)) = 1 \tag{14}$$

with $M_{ij}(z_j(t))$ being the grade of membership of $z_j(t)$ in M_{ij}. $h_i(z(t))$ can be regarded as the normalized weights of the IF-THEN rules.

4.2. T-S Fuzzy Controller Design Based on LMI

Rule R^i is as follows: IF $z_1(t)$ is M_{i1} and $\cdots$ and $z_n(t)$ is M_{in}

$$\text{THEN } u(t) = K_i x(t) \quad (i = 1, 2, \ldots, r). \tag{15}$$

The inferred output of the PDC controller is expressed in the following form:

$$u(t) = \sum_{j=1}^{r} h_j(z(t)) K_j x(t), \tag{16}$$

where K_j represents the feedback gain.

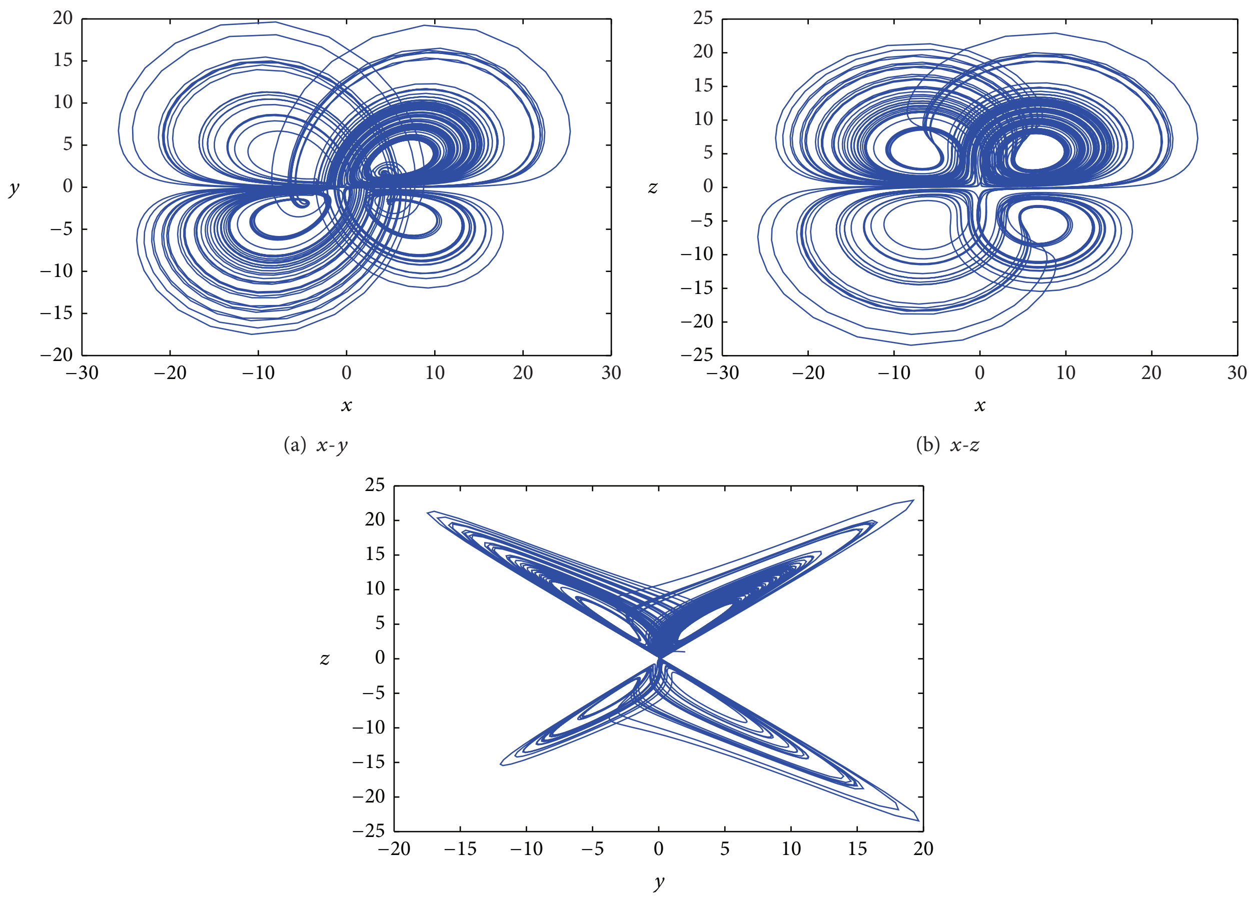

(a) x-y

(b) x-z

(c) y-z

FIGURE 2: Phase trajectories of wing doubled fractional-order chaotic system (8).

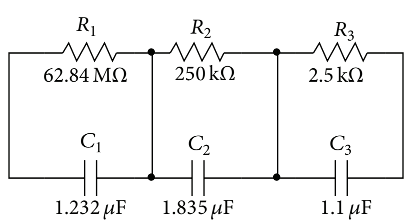

FIGURE 3: The unit circuit of $1/s^{0.9}$.

By substituting (16) into (13), one has

$$\frac{d^q x}{dt^q} = \sum_{i=1}^{r} h_i(z(t)) A_i x(t) + \sum_{i=1}^{r} h_i(z(t)) B_i \sum_{j=1}^{r} h_j(z(t)) K_j x(t). \tag{17}$$

In order to simplify (17), it is modified as follows:

$$\sum_{i=1}^{r} h_i A_i = h_1 A_1 + h_2 A_2 + \cdots + h_r A_r. \tag{18}$$

Considering $\sum_{i=1}^{r} h_i(z(t)) = 1$ in (17), (18) can be written as

$$\begin{aligned}\sum_{i=1}^{r} h_i A_i &= h_1 (h_1 + h_2 + \cdots + h_r) A_1 + \cdots \\ &\quad + h_r (h_1 + h_2 + \cdots + h_r) A_r \\ &= (h_1{}^2 + h_1 h_2 + \cdots + h_1 h_r) A_1 + \cdots \\ &\quad + (h_r h_1 + h_r h_2 + \cdots + h_r{}^2) A_r \\ &= \sum_{i=1}^{r}\sum_{j=1}^{r} h_i h_j A_i.\end{aligned} \tag{19}$$

For formula (17), $\sum_{i=1}^{r} h_i B_i \sum_{j=1}^{r} h_j K_j$ can be written as

$$\begin{aligned}\sum_{i=1}^{r} h_i B_i \sum_{j=1}^{r} h_j K_j &= (h_1 B_1 + h_2 B_2 + \cdots + h_r B_r) \\ &\quad \cdot (h_1 K_1 + h_2 K_2 + \cdots + h_r K_r) \\ &= h_1 B_1 (h_1 K_1 + \cdots + h_r K_r) + \cdots \\ &\quad + h_r B_r (h_1 K_1 + h_2 K_2 + \cdots + h_r K_r) = h_1{}^2 B_1 K_1\end{aligned}$$

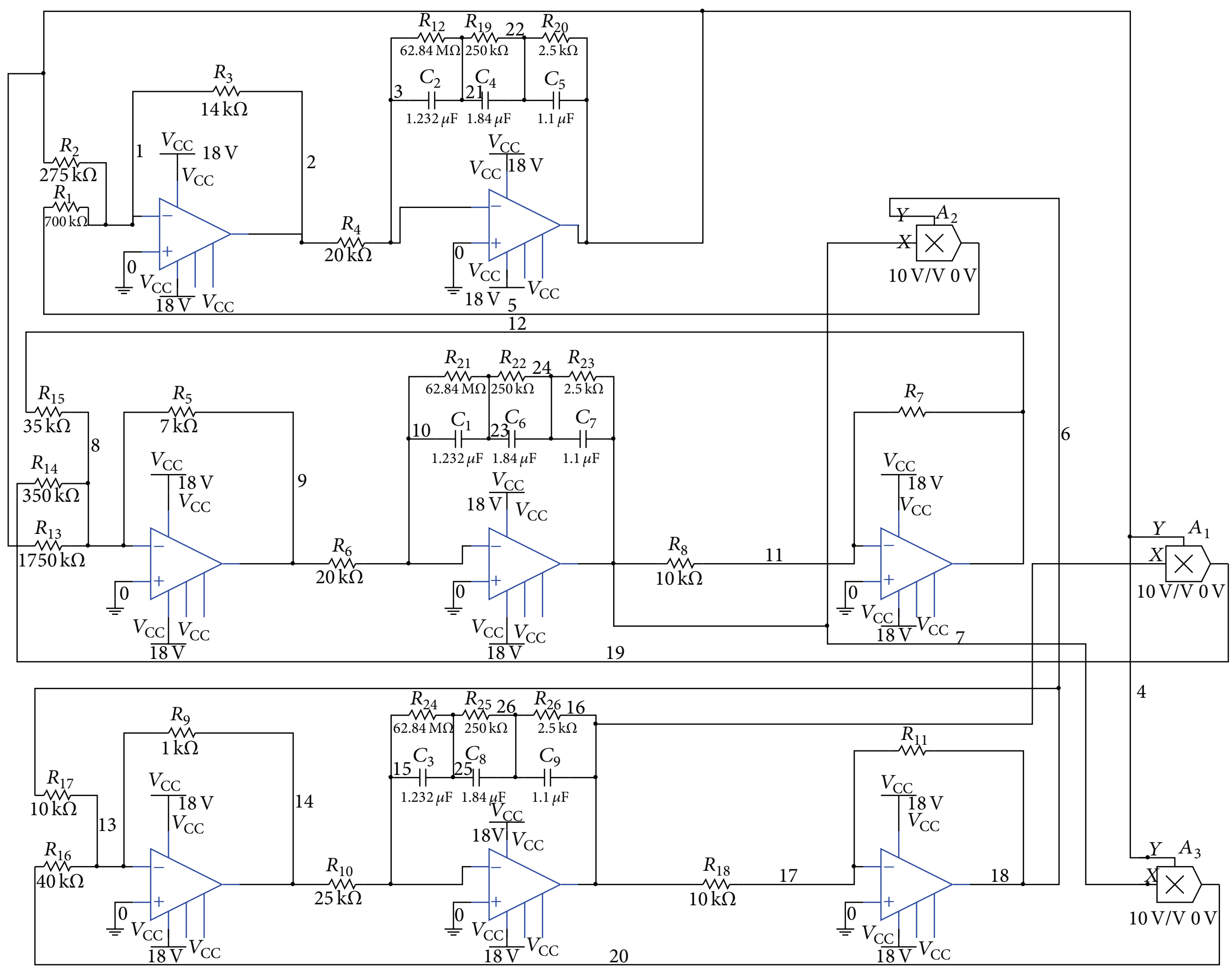

Figure 4: Circuit diagram to realize the new fractional-order chaotic system (5).

$$
\begin{aligned}
&+h_2{}^2B_2K_2+\cdots+h_i{}^2B_iK_i+\cdots+h_r{}^2B_rK_r\\
&+h_1\left(h_2K_2+h_3K_3+\cdots+h_rK_r\right)B_1\\
&+h_2\left(h_3K_3+\cdots+h_rK_r\right)B_2+\cdots\\
&+h_i\left(h_{i+1}K_{i+1}+\cdots+h_rK_r\right)B_i+\cdots\\
&+h_{r-1}h_rK_rB_{r-1}+h_2h_1K_1B_2+h_3\left(h_2K_2+h_1K_1\right)\\
&\cdot B_3+\cdots+h_j\left(h_{j-1}K_{j-1}+h_{j-2}K_{j-2}+\cdots+h_1K_1\right)\\
&\cdot B_j+\cdots+h_r\left(h_{r-1}K_{r-1}+h_{r-2}K_{r-2}+\cdots+h_1K_1\right)\\
&\cdot B_r=\sum_{i=1}^{r}h_i{}^2B_iK_j+\sum_{i<j}^{r}h_ih_jK_jB_i+\sum_{i>j}^{r}h_ih_jK_jB_i\\
&=\sum_{i=1}^{r}\sum_{j=1}^{r}h_ih_jB_iK_j.
\end{aligned}
\tag{20}
$$

Submitting (19) and (20) into (17), one gets

$$\frac{d^q x}{dt^q}=\sum_{i=1}^{r}\sum_{j=1}^{r}h_i\left(z\left(t\right)\right)h_j\left(z\left(t\right)\right)\left(A_i+B_iK_j\right)x\left(t\right). \tag{21}$$

Before utilizing the T-S fuzzy model into fractional-order systems (5) and (8), make the following assumptions.

Assumption 5. According to the boundedness of the system, the scope of the system state can be defined as

$$
\begin{gathered}
\Omega\equiv\left\{x\left(t\right)\in R\mid\left\|x\left(t\right)\right\|^n\leq\delta\right\},\\
x_i\left(t\right)\in\left[-d_i,d_i\right],\ d_i>0\ \ (i=1,2).
\end{gathered}
\tag{22}
$$

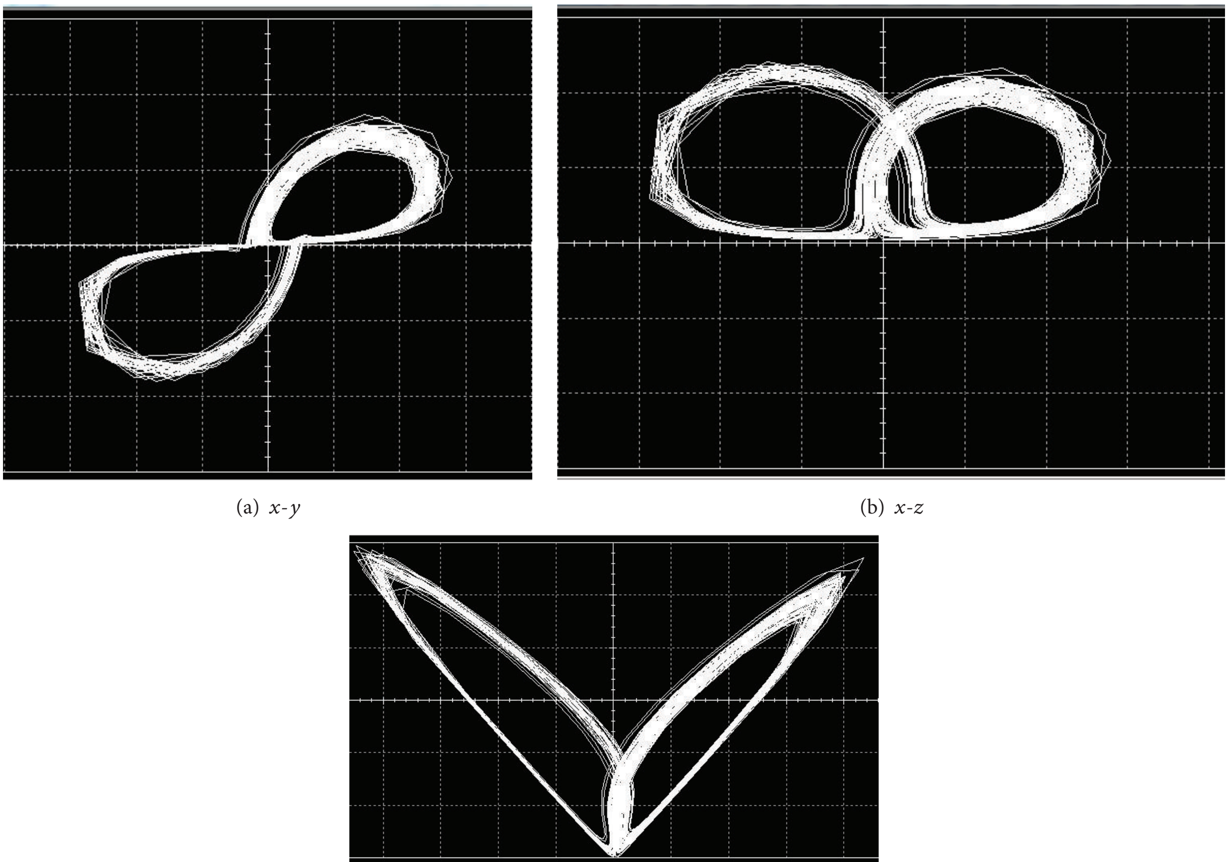

(a) x-y

(b) x-z

(c) y-z

Figure 5: Circuit simulation results of the new fractional-order chaotic system (5).

Assumption 6. The feedback control can be applied to every state of the system. The PDC approach together with the T-S fuzzy model can be adopted to control systems (5) and (8).

Based on the above assumptions, we can use T-S fuzzy model to describe system (5). Suppose that $x_1(t) \in [-d_1, d_1]$, $x_2(t) \in [-d_2, d_2]$, where $d_1 = 15$ and $d_2 = 10$.

Thus, the T-S fuzzy model can be presented as follows:

R^1: IF $x_1(t)$ is $M_1(x_1(t))$, THEN $d^q x/dt^q = A_1 x(t) + B_1 u(t)$,

R^2: IF $x_1(t)$ is $M_2(x_1(t))$, THEN $d^q x/dt^q = A_2 x(t) + B_2 u(t)$,

R^3: IF $x_2(t)$ is $M_3(x_2(t))$, THEN $d^q x/dt^q = A_3 x(t) + B_3 u(t)$,

R^4: IF $x_2(t)$ is $M_4(x_2(t))$, THEN $d^q x/dt^q = A_4 x(t) + B_4 u(t)$,

where $x(t) = [x_1(t), x_2(t), x_3(t)]^T$, $u(t) = [u_1(t), u_2(t), u_3(t)]^T$,

$$
\begin{gathered}
A_1 = \begin{bmatrix} \frac{28}{11} & 0 & 0 \\ 0.2 & -10 & 15 \\ 0 & 15 & -4 \end{bmatrix}, \\
A_2 = \begin{bmatrix} \frac{28}{11} & 0 & 0 \\ 0.2 & -10 & -15 \\ 0 & -15 & -4 \end{bmatrix}, \\
A_3 = \begin{bmatrix} \frac{28}{11} & 0 & -10 \\ 0.2 & -10 & 0 \\ 10 & 0 & -4 \end{bmatrix}, \\
A_4 = \begin{bmatrix} \frac{28}{11} & 0 & 10 \\ 0.2 & -10 & 0 \\ -10 & 0 & -4 \end{bmatrix}, \\
B_1 = B_2 = B_3 = B_4 = I_{3\times 3} \quad (I \text{ is a unit matrix}).
\end{gathered}
\tag{23}
$$

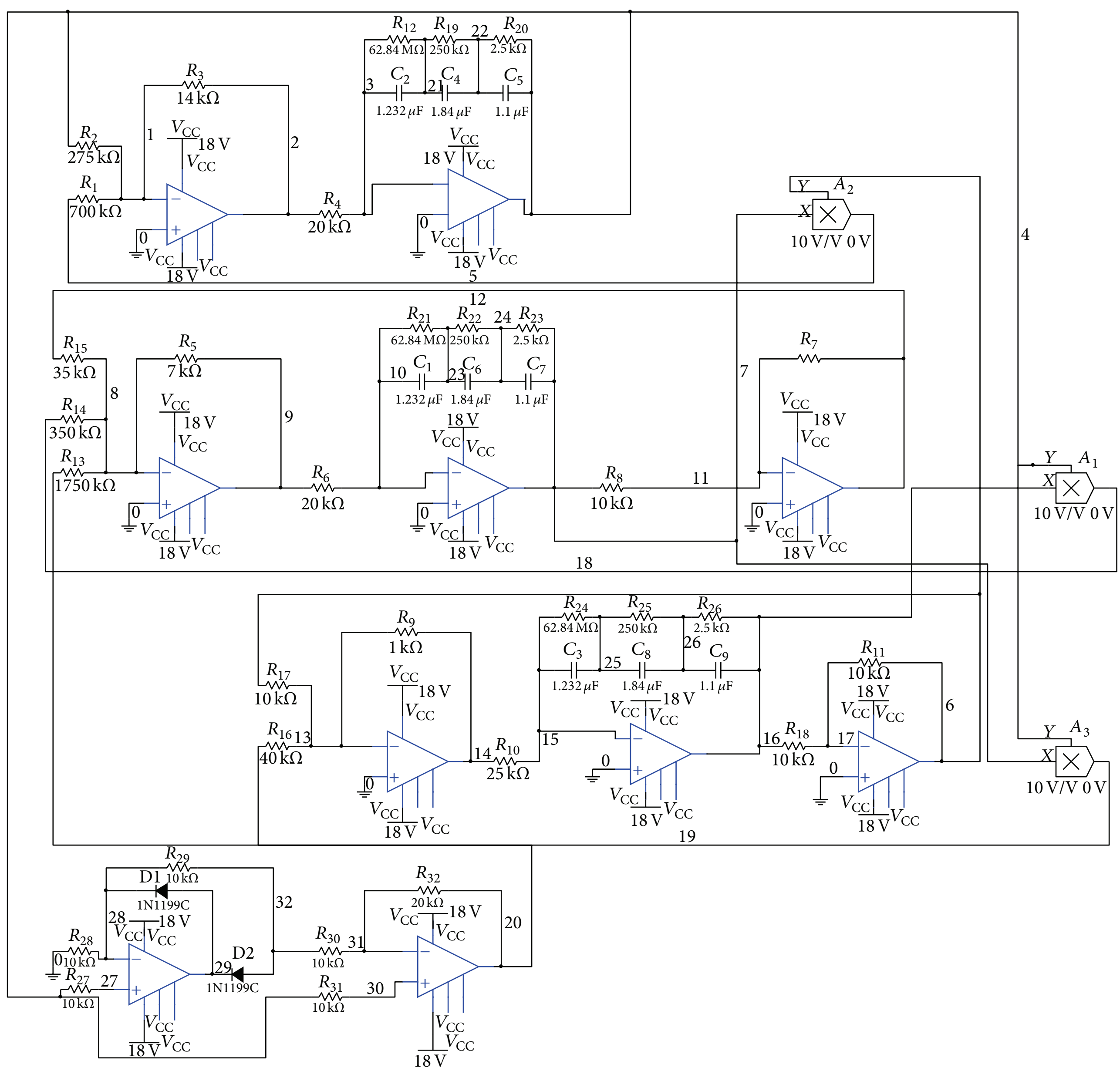

Figure 6: Circuit diagram to realize the new wing doubled fractional-order chaotic system (8).

The membership functions of fuzzy sets are taken as follows:

$$M_1(x_1(t)) = \frac{1}{2}\left(1 + \frac{x_1(t)}{d_1}\right),$$
$$M_2(x_1(t)) = \frac{1}{2}\left(1 - \frac{x_1(t)}{d_1}\right),$$
$$M_3(x_2(t)) = \frac{1}{2}\left(1 + \frac{x_2(t)}{d_2}\right),$$
$$M_4(x_2(t)) = \frac{1}{2}\left(1 - \frac{x_2(t)}{d_2}\right). \tag{24}$$

Thus, the fractional-order system (5) based on T-S fuzzy model can be expressed as

$$\frac{d^q x}{dt^q} = \sum_{i=1}^{4} h_i(z(t))\left(A_i x(t) + B_i u(t)\right). \tag{25}$$

According to the PDC method, the controller is given as follows:

$$R^1\text{: IF } x_1(t) \text{ is } M_1(x_1(t))\text{, THEN } u(t) = K_1 x(t),$$
$$R^2\text{: IF } x_1(t) \text{ is } M_2(x_1(t))\text{, THEN } u(t) = K_2 x(t),$$
$$R^3\text{: IF } x_2(t) \text{ is } M_3(x_2(t))\text{, THEN } u(t) = K_3 x(t),$$
$$R^4\text{: IF } x_2(t) \text{ is } M_4(x_2(t))\text{, THEN } u(t) = K_4 x(t).$$

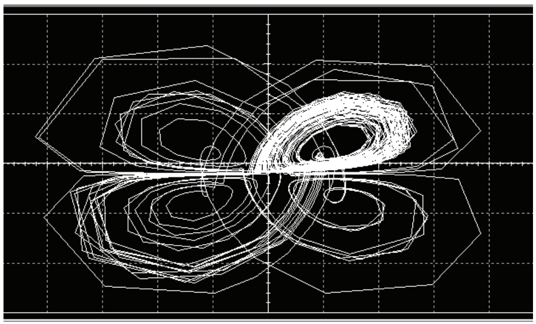

(a) x-y

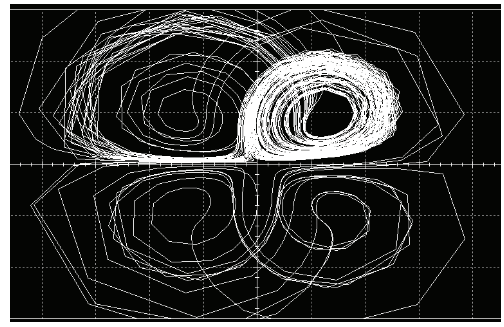

(b) x-z

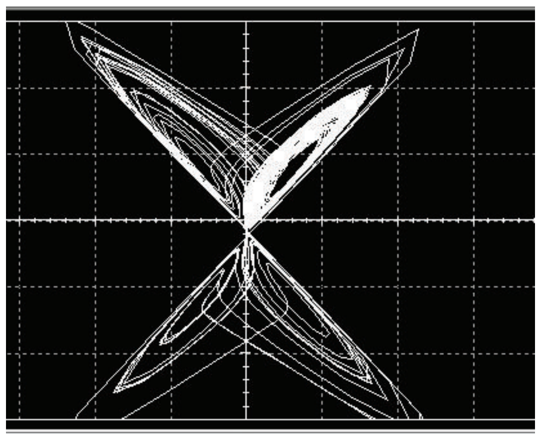

(c) y-z

Figure 7: Circuit simulation results of the new wing doubled fractional-order chaotic system (8).

The overall controller is obtained as

$$u(t)=\sum_{j=1}^{4}h_j(z(t))K_jx(t). \tag{26}$$

Submitting (26) into (25), one can get the fractional-order system:

$$\frac{d^qx}{dt^q}=\sum_{i=1}^{4}\sum_{j=1}^{4}h_i(z(t))h_j(z(t))\left(A_i+B_iK_j\right)x(t). \tag{27}$$

Similarly, for wing doubled system (8), $d_1=30$ and $d_2=20$. One has

$$\begin{gathered}A_1=\begin{bmatrix}\frac{28}{11}&0&0\\0&-10&30\\0&30&-4\end{bmatrix},\\ A_2=\begin{bmatrix}\frac{28}{11}&0&0\\0&-10&-30\\0&-30&-4\end{bmatrix},\\ A_3=\begin{bmatrix}\frac{28}{11}&0&-20\\0&-10&0\\20&0&-4\end{bmatrix},\\ A_4=\begin{bmatrix}\frac{28}{11}&0&20\\0&-10&0\\-20&0&-4\end{bmatrix}.\end{gathered} \tag{28}$$

To stabilize the fractional-order system (27), the following lemma and theorem are given.

Lemma 7 (see [27]). *For the arbitrary state variable $x=[x_1,x_2,\dots,x_n]^T$, if there exists a symmetric positive definite real matrix P satisfying $J=x^TP(d^qx/dt^q)\le 0$ ($x^TP(d^qx/dt^q)$ is called J function), then the fractional-order system (27) is globally asymptotically stable. Condition*

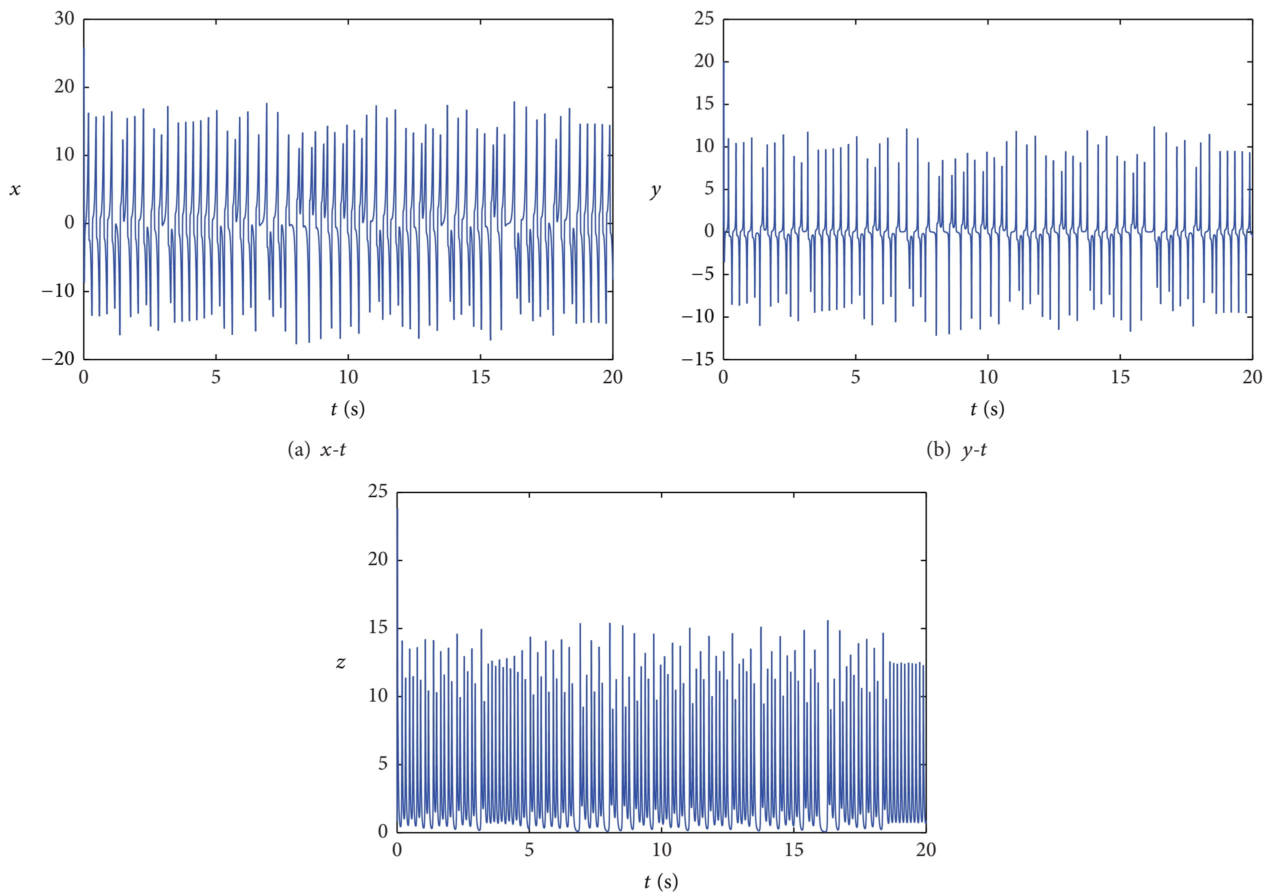

(a) x-t

(b) y-t

(c) z-t

Figure 8: State trajectories of system (5) without controller.

$J = x^T P(d^q x/dt^q) \le 0$ can be equally written as $J_0 = x^T P(d^q x/dt^q) + (d^q x/dt^q)^T Px \le 0$.

Theorem 8. *If there exist positive definite matrices P, E, and F as well as a positive constant η, suppose that λ_i $(i = 1, 2, 3, 4)$ and ξ_i $(i = 1, 2, 3, 4)$ are the eigenvalues of matrices $PEE^T P$ and $F^T F$, respectively. If λ_i $(i = 1, 2, 3, 4) > 0$, ξ_i $(i = 1, 2, 3, 4) > 0$, and we select the controller gain matrix K_i $(i = 1, 2, 3, 4)$ which satisfies the following inequalities, the fractional-order system (27) is globally asymptotically stable:*

$$G_{ii}{}^T P + PG_{ii} + \eta PEE^T P + \eta^{-1} F^T F < 0 \quad (i, j = 1, 2, 3, 4), \tag{29}$$

$$G_{ij}{}^T P + PG_{ij} + \eta PEE^T P + \eta^{-1} F^T F < 0 \quad (i < j < 4), \tag{30}$$

where $G_{ii} = A_i + B_i K_i$ and $G_{ij} = ((A_i + B_i K_j) + (A_j + B_j K_i))/2$.

Proof. By Lemma 7, select $J_0 = x^T P(d^q x/dt^q) + (d^q x/dt^q)^T Px$ as J function of system (27):

$$\begin{aligned}
J_0 &= x^T P \frac{d^q x}{dt^q} + \left(\frac{d^q x}{dt^q}\right)^T Px \\
&= x^T P \sum_{i=1}^{4}\sum_{j=1}^{4} h_i h_j \left(A_i + B_i K_j\right) x \\
&\quad + \sum_{i=1}^{4}\sum_{j=1}^{4} h_i h_j \left(A_i + B_i K_j\right)^T Px \\
&= \sum_{i=1}^{4}\sum_{j=1}^{4} h_i h_j x^T \left[\left(A_i + B_i K_j\right)^T P + P\left(A_i + B_i K_j\right)\right] x \\
&= \sum_{i=1}^{4} h_i^2 x^T \left[\left(A_i + B_i K_i\right)^T P + P\left(A_i + B_i K_i\right)\right] x \\
&\quad + \sum_{i<j}^{4} h_i h_j x^T \left[\left(A_i + B_i K_j\right)^T P + P\left(A_i + B_i K_j\right)\right] x \\
&\quad + \sum_{i>j}^{4} h_i h_j x^T \left[\left(A_i + B_i K_j\right)^T P + P\left(A_i + B_i K_j\right)\right] x.
\end{aligned} \tag{31}$$

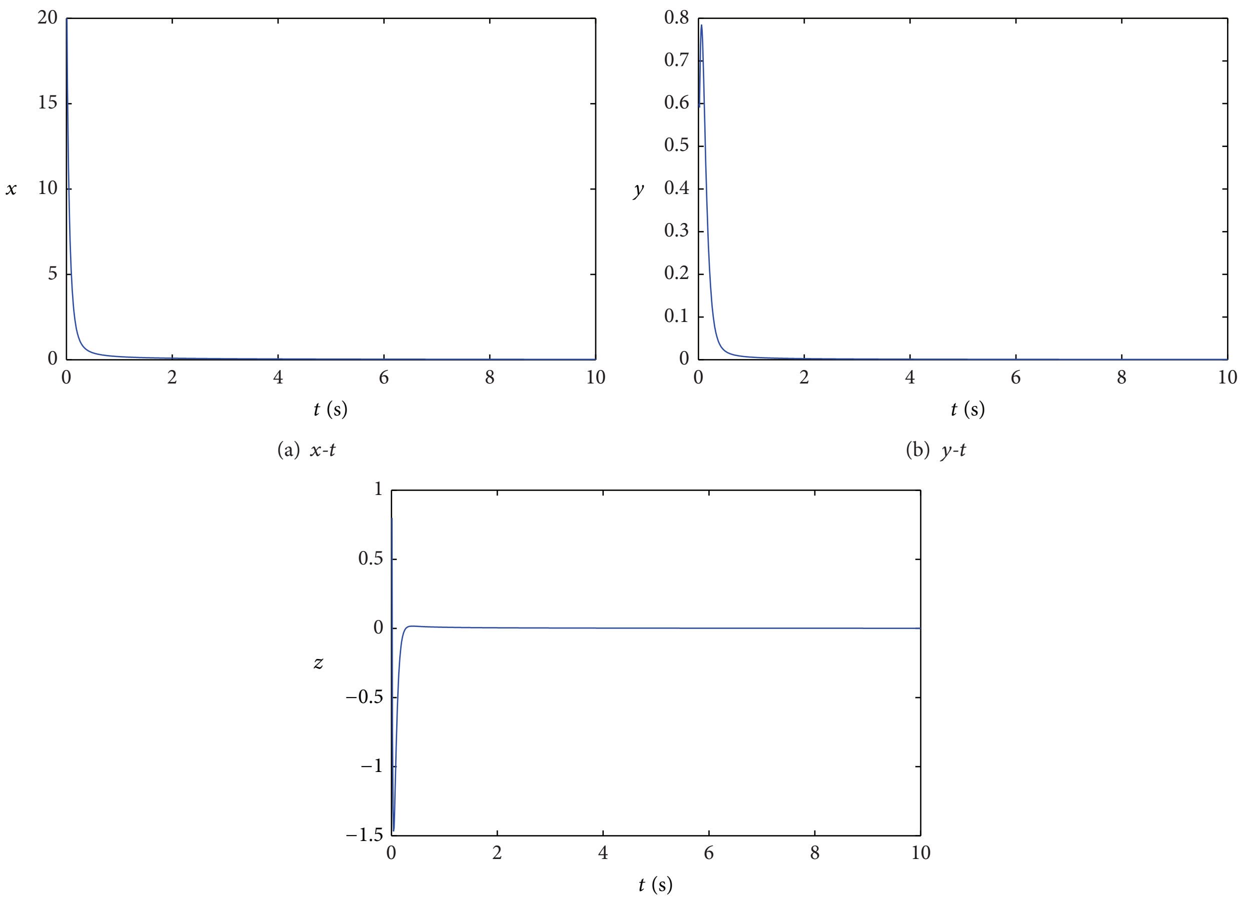

(a) x-t

(b) y-t

(c) z-t

FIGURE 9: State trajectories of closed-loop system (5) with controller (26).

According to $\sum_{i=1}^{4} h_i^{\,2} + 2\sum_{i<j}^{4} h_i h_j = 1$ in (14), so there is

$$\begin{aligned}
&\sum_{i<j}^{4} h_i h_j x^T \left[\left(A_i + B_i K_j\right)^T P + P\left(A_i + B_i K_j\right)\right] x \\
&\quad + \sum_{i>j}^{4} h_i h_j x^T \left[\left(A_i + B_i K_j\right)^T P + P\left(A_i + B_i K_j\right)\right] x \\
&\quad = \sum_{i<j}^{4} h_i h_j x^T \left\{\left[\left(A_i + B_i K_j\right) + \left(A_j + B_j K_i\right)\right]^T P\right. \\
&\quad \left. + P\left[\left(A_i + B_i K_j\right) + \left(A_j + B_j K_i\right)\right]\right\} x \\
&\quad = 2\sum_{i<j}^{4} h_i h_j x^T \left\{\left[\frac{\left(A_i + B_i K_j\right) + \left(A_j + B_j K_i\right)}{2}\right]^T P\right. \\
&\quad \left. + P\left[\frac{\left(A_i + B_i K_j\right) + \left(A_j + B_j K_i\right)}{2}\right]\right\} x.
\end{aligned} \tag{32}$$

Selecting $G_{ii} = A_i + B_i K_i$, $G_{ij} = ((A_i + B_i K_j) + (A_j + B_j K_i))/2$ and under conditions (29) and (30), one gets

$$\begin{aligned}
J_0 &= \sum_{i=1}^{4} h_i^2 x^T \left(G_{ii}{}^T P + P G_{ii}\right) x \\
&\quad + 2\sum_{i<j}^{4} h_i h_j x^T \left(G_{ij}{}^T P + P G_{ij}\right) < x \\
&\quad - \left\{\sum_{i=1}^{4} h_i^{\,2} x^T \left(\eta P E E^T P + \eta^{-1} F^T F\right) x\right. \\
&\quad \left. + 2\sum_{i<j}^{4} h_i h_j x^T \left(\eta P E E^T P + \eta^{-1} F^T F\right) x\right\}.
\end{aligned} \tag{33}$$

According to Theorem 4, the eigenvalues of the matrices PEE^TP and F^TF are λ_i $(i = 1, 2, 3, 4) > 0$ and ξ_i $(i = 1, 2, 3, 4) > 0$, respectively, so the matrices PEE^TP and F^TF

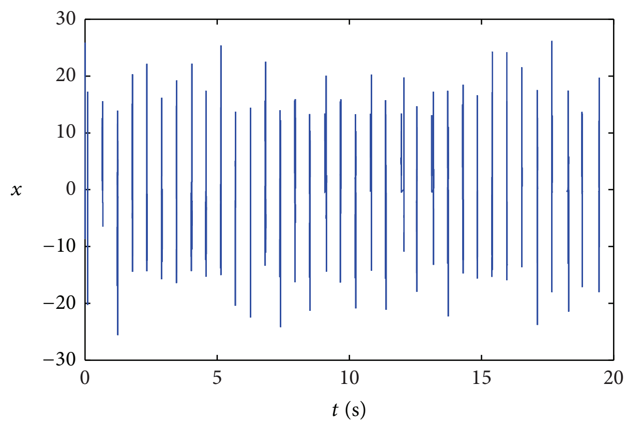

(a) x-t

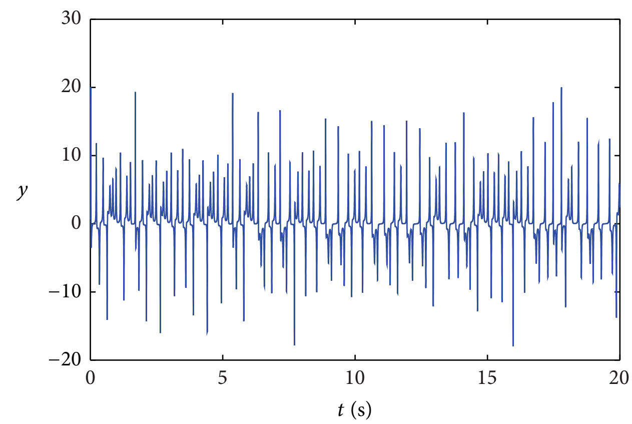

(b) y-t

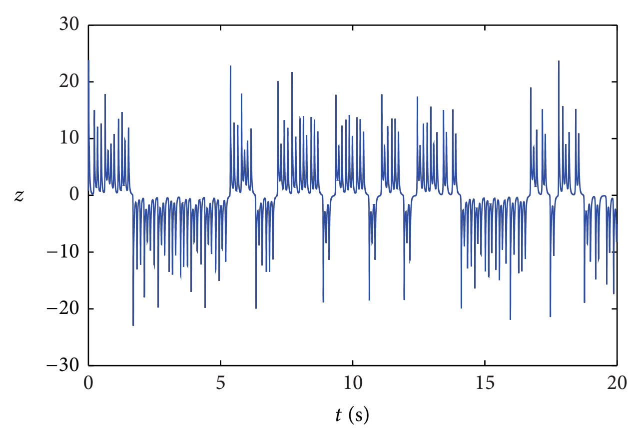

(c) z-t

Figure 10: State trajectories of system (8) without controller.

both are positive definite matrix; that is, $PEE^TP + F^TF > 0$; since $\eta > 0$, one gets

$$\eta PEE^TP + \eta^{-1}F^TF > 0. \tag{34}$$

Considering (34) for (33), one can get

$$\begin{aligned} J_0 < -\Bigg\{ &\sum_{i=1}^{4} {h_i}^2 x^T \left(\eta PEE^TP + \eta^{-1}F^TF\right) x \\ &+ 2\sum_{i<j}^{4} h_i h_j x^T \left(\eta PEE^TP + \eta^{-1}F^TF\right) x \Bigg\} < 0. \end{aligned} \tag{35}$$

Therefore, when inequalities (29) and (30) hold, one has

$$J_0 = x^T P \frac{d^q x}{dt^q} + \left(\frac{d^q x}{dt^q}\right)^T Px \leq 0. \tag{36}$$

This shows that the fractional system (27) is globally asymptotically stable. This completes the proof. □

According to Schur complement theorem, inequalities (29) and (30) can be transformed into the problem of solving linear matrix inequalities (LMIs).

From (29), we can obtain

$$\begin{aligned} &A_i^TP + {K_i}^TB_iP + PA_i + PB_iK_i + \eta PEE^TP + \eta^{-1}F^TF \\ &\quad < 0. \end{aligned} \tag{37}$$

Multiplying P^{-1} both in the left and in the right in (37), one gets

$$\begin{aligned} &P^{-1}A_i^T + P^{-1}K_i^TB_i + A_iP^{-1} + B_iK_iP^{-1} + \eta EE^T \\ &\quad + \eta^{-1}P^{-1}F^TFP^{-1} < 0. \end{aligned} \tag{38}$$

In (38), selecting $Q = P^{-1}$ and $M_i = K_iP^{-1}$, we can obtain

$$\begin{aligned} &QA_i^T + A_iQ + M_i^TB_i^T + B_iM_i + \eta EE^T + \eta^{-1}QF^TFQ \\ &\quad < 0. \end{aligned} \tag{39}$$

The controller gain is $K_i = M_iQ^{-1}$.

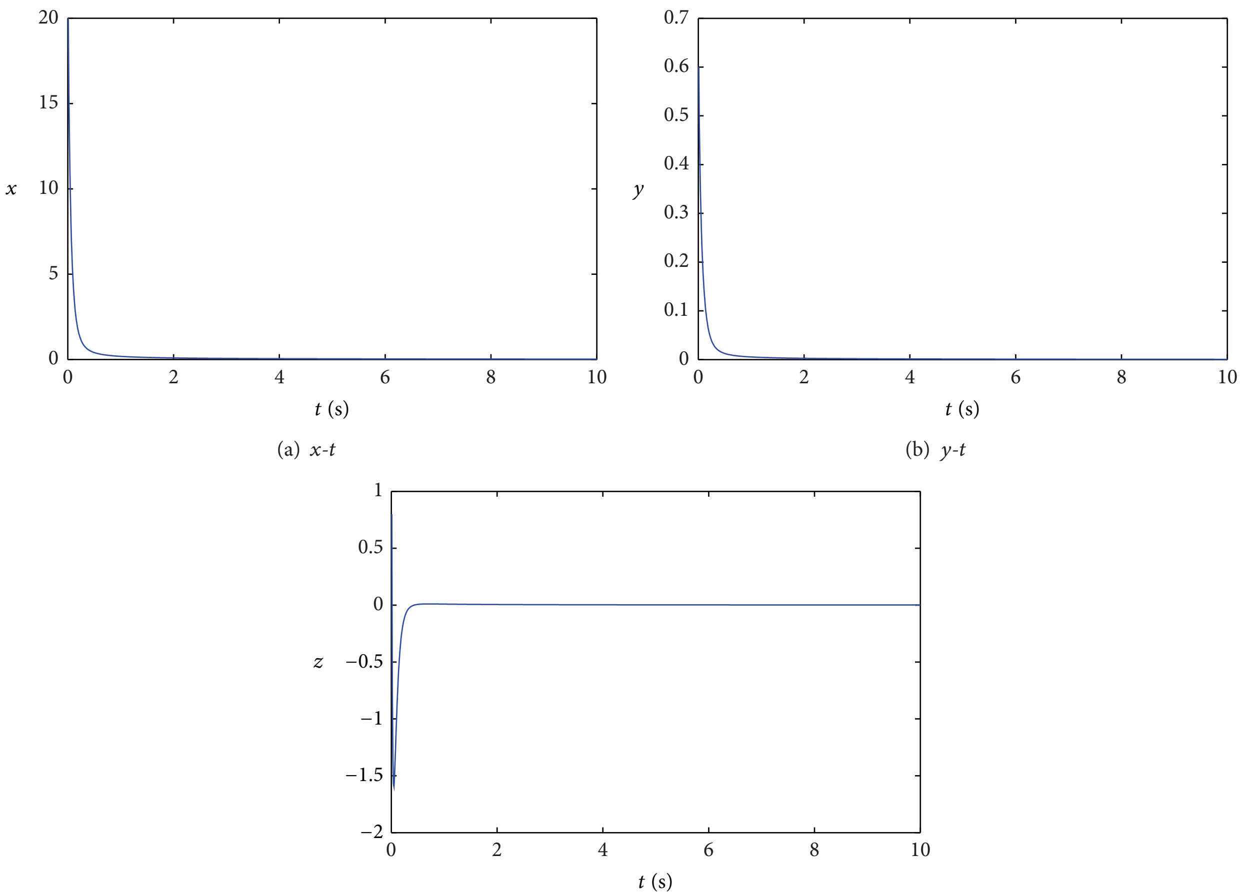

(a) x-t

(b) y-t

(c) z-t

FIGURE 11: State trajectories of closed-loop system (8) with controller (26).

From (30), we can obtain

$$\frac{1}{2}\left(A_i^T P + K_j^T B_i^T P + A_j^T P + K_i^T B_j^T P + PA_i + PB_iK_j + PA_j + PB_jK_i\right) + \eta PEE^T P + \eta^{-1} F^T F < 0. \tag{40}$$

Multiplying P^{-1} both in the left and in the right in (40), we obtain

$$\frac{1}{2}\left(P^{-1}A_i^T + P^{-1}K_j^T B_i^T + P^{-1}A_j^T + P^{-1}K_i^T B_j^T + A_iP^{-1} + B_iK_jP^{-1} + A_jP^{-1} + B_jK_iP^{-1}\right) + \eta EE^T + \eta^{-1}P^{-1}F^T FP^{-1} < 0. \tag{41}$$

In (41), selecting $Q = P^{-1}$, $M_i = K_iP^{-1}$, and $M_j = K_jP^{-1}$, we can obtain

$$\frac{1}{2}\left(QA_i^T + A_iQ + M_i^T B_j^T + B_jM_i + QA_j^T + A_jQ + M_j^T B_i^T + B_iM_j\right) + \eta EE^T + \eta^{-1}QF^T FQ < 0. \tag{42}$$

The controller gain is $K_i = M_iQ^{-1}$.

By Schur complement theorem, (39) can be written as

$$\begin{bmatrix} QA_i^T + M_i^T B_i^T + A_iQ + B_iM_i + \eta EE^T & QF^T \\ FQ & -\eta^{-1}I \end{bmatrix} < 0. \tag{43}$$

Similarly, (42) can be written as

$$\begin{bmatrix} \frac{1}{2}\left(QA_i^T + A_i^TQ + M_i^T B_j^T + B_jM_i + QA_j^T + A_j^TQ + M_j^T B_i^T + B_iM_j\right) + \eta EE^T & QF^T \\ FQ & -\eta^{-1}I \end{bmatrix} < 0 \tag{44}$$

$$Q > 0.$$

For a given positive number $\eta > 0$, we can use Matlab LMI toolbox to solve the linear matrix inequalities (43) and (44) to obtain the positive definite matrix P and the controller gain K_i $(i = 1, 2, 3, 4)$.

4.3. Simulation Results. For fractional-order system (5), take $d_1 = 15$, $d_2 = 10$, and $\eta = 10000$. According to Theorem 4, select positive definite matrices:

$$\begin{aligned} E &= [1\ 0\ 0\ 0\ 0\ 0\ 0\ 0\ 0;\ 0\ 1\ 0\ 0\ 0\ 0\ 0\ 0\ 0;\ 0\ 0\ 1\ 0\ 0\ 0\ 0\ 0\ 0]; \\ F &= [1\ 0\ 0; 0\ 1\ 0; 0\ 0\ 1;\ 1\ 0\ 0; 0\ 1\ 0; 0\ 0\ 1;\ 1\ 0\ 0; 0\ 1\ 0; 0\ 0\ 1]. \end{aligned} \tag{45}$$

Through Matlab 7.0 LMI toolbox, the positive definite matrix P and the feedback controller gain K_i $(i = 1, 2, 3, 4)$ can be obtained:

$$\begin{aligned} P &= \operatorname{diag}(0.00066, 0.00066, 0.00066), \\ K_1 &= \begin{bmatrix} -9.2609 & -0.0583 & 0.1021 \\ -0.1417 & 3.2846 & -22.0523 \\ -0.1021 & -7.9477 & -2.7154 \end{bmatrix}, \\ K_2 &= \begin{bmatrix} -9.2609 & -0.1217 & 0.0497 \\ -0.0783 & 3.2846 & 11.4239 \\ -0.0497 & 18.5761 & -2.7154 \end{bmatrix}, \\ K_3 &= \begin{bmatrix} -9.2609 & -0.1278 & -0.2628 \\ -0.0722 & 3.2846 & -0.0017 \\ 0.2628 & 0.0017 & -2.7154 \end{bmatrix}, \\ K_4 &= \begin{bmatrix} -9.2609 & -0.1234 & -0.1296 \\ -0.0766 & 3.2846 & -0.0068 \\ 0.1296 & 0.0068 & -2.7154 \end{bmatrix}. \end{aligned} \tag{46}$$

Substituting the value of K_i $(i = 1, 2, 3, 4)$ into (26), the desired feedback controller $u(t)$ can be got. Figure 8 shows the state trajectories of system (5) without controller; the system states are unstable. Figure 9 illustrates the state trajectories of closed-loop system (5) with controller (26), and the states of system (5) globally converge to the equilibrium point which implies the effectiveness of the designed controller.

Similarly, for wing doubled system (8), select $d_1 = 30$, $d_2 = 20$, and $\eta = 10000$. According to Theorem 4, take positive definite matrices:

$$\begin{aligned} E &= [1\ 0\ 0\ 0\ 0\ 0\ 0\ 0\ 0;\ 0\ 1\ 0\ 0\ 0\ 0\ 0\ 0\ 0;\ 0\ 0\ 1\ 0\ 0\ 0\ 0\ 0\ 0]; \\ F &= [1\ 0\ 0; 0\ 1\ 0; 0\ 0\ 1;\ 1\ 0\ 0; 0\ 1\ 0; 0\ 0\ 1;\ 1\ 0\ 0; 0\ 1\ 0; 0\ 0\ 1]. \end{aligned} \tag{47}$$

Through Matlab LMI toolbox, the positive definite matrix P and the feedback controller gain K_i $(i = 1, 2, 3, 4)$ can be obtained:

$$\begin{aligned} P &= \operatorname{diag}(0.00066, 0.00066, 0.00066) \\ K_1 &= \begin{bmatrix} -9.2609 & 0.0056 & 0.0005 \\ -0.0056 & 3.2846 & -30.4410 \\ -0.0005 & -29.5590 & -2.7154 \end{bmatrix}, \\ K_2 &= \begin{bmatrix} -9.2609 & -0.0091 & 0.0002 \\ 0.0091 & 3.2846 & 30.1005 \\ -0.0002 & 29.8995 & -2.7154 \end{bmatrix}, \\ K_3 &= \begin{bmatrix} -9.2609 & -0.0000 & -0.7819 \\ 0.0000 & 3.2846 & -0.0000 \\ 0.7819 & 0.0000 & -2.7154 \end{bmatrix}, \\ K_4 &= \begin{bmatrix} -9.2609 & -0.0000 & 0.0255 \\ 0.0000 & 3.2846 & -0.0000 \\ -0.0255 & 0.0000 & -2.7154 \end{bmatrix}. \end{aligned} \tag{48}$$

Substituting the value of K_i $(i = 1, 2, 3, 4)$ into (26), the controller can be got. Figure 10 shows the state trajectories of system (8) without controller; the system states are unstable. Figure 11 illustrates the state trajectories of system (8) with controller (26). We can see that the controller can be applied to the more complicated wing doubled chaotic system (8) with short time and small overshoot, which shows the speed ability and robustness of the control method.

5. Conclusions

A new three-dimensional fractional-order chaos was proposed in this paper. When the linear term x in the second equation of the system was replaced by its absolute value, the new system can make the wing of the original system doubled, and the circuit diagram was implemented. Based on the T-S fuzzy model and fractional-order stability theory, a more practical stability condition for fuzzy control of the proposed wing doubled fractional-order chaos was given as a set of LMI and the strict mathematical derivation was presented. Numerical simulation results were consistent with theoretical results.

More and better methods for the control of fractional-order chaotic systems should be studied. The authors will continue the study of application condition of integer-order chaotic theory into fractional-order chaotic systems. There will be focus on the stability of fractional-order chaotic systems.

Conflict of Interests

The authors declare that there is no conflict of interests regarding the publication of this paper.

Acknowledgments

This work was supported by the "948" Project from the Ministry of Water Resources of China (Grant no. 201436), the 111 Project from the Ministry of Education of China (no. B12007), and Yangling Demonstration Zone Technology Project (2014NY-32).

References

[1] M. R. Peterson and C. Nayak, "Effects of landau level mixing on the fractional quantum hall effect in monolayer graphene," *Physical Review Letters*, vol. 113, no. 8, Article ID 086401, 2014.

[2] G. Maione, "On the Laguerre rational approximation to fractional discrete derivative and integral operators," *IEEE Transactions on Automatic Control*, vol. 58, no. 6, pp. 1579–1585, 2013.

[3] B. E. Feldman, B. Krauss, J. H. Smet, and A. Yacoby, "Unconventional sequence of fractional quantum hall states in suspended graphene," *Science*, vol. 337, no. 6099, pp. 1196–1199, 2012.

[4] X.-Y. Wang and M.-J. Wang, "Dynamic analysis of the fractional-order Liu system and its synchronization," *Chaos*, vol. 17, no. 3, Article ID 033106, 2007.

[5] D. Y. Chen, R. F. Zhang, X. Z. Liu, and X. Y. Ma, "Fractional order Lyapunov stability theorem and its applications in synchronization of complex dynamical networks," *Communications in Nonlinear Science and Numerical Simulation*, vol. 19, no. 12, pp. 4105–4121, 2014.

[6] R. X. Zhang and S. P. Yang, "Stabilization of fractional-order chaotic system via a single state adaptive-feedback controller," *Nonlinear Dynamics*, vol. 68, no. 1-2, pp. 45–51, 2012.

[7] C. X. Liu and J. J. Lu, "A novel fractional-order hyperchaotic system and its circuit realization," *International Journal of Modern Physics B*, vol. 24, no. 10, pp. 1299–1307, 2010.

[8] S. Ghasemi, A. Tabesh, and J. Askari-Marnani, "Application of fractional calculus theory to robust controller design for wind turbine generators," *IEEE Transactions on Energy Conversion*, vol. 29, no. 3, pp. 780–787, 2014.

[9] L. Teng, H. H. C. Iu, X. Y. Wang, and X. K. Wang, "Chaotic behavior in fractional-order memristor-based simplest chaotic circuit using fourth degree polynomial," *Nonlinear Dynamics*, vol. 77, no. 1-2, pp. 231–241, 2014.

[10] Y. Chai, L. P. Chen, R. C. Wu, and J. Sun, "Adaptive pinning synchronization in fractional-order complex dynamical networks," *Physica A: Statistical Mechanics and Its Applications*, vol. 391, no. 22, pp. 5746–5758, 2012.

[11] A. Flores-Tlacuahuac and L. T. Biegler, "Optimization of fractional order dynamic chemical processing systems," *Industrial and Engineering Chemistry Research*, vol. 53, no. 13, pp. 5110–5127, 2014.

[12] G. H. Sun, M. Wang, L. L. Huang, and L. Q. Shen, "Generating multi-scroll chaotic attractors via switched fractional systems," *Circuits, Systems, and Signal Processing*, vol. 30, no. 6, pp. 1183–1195, 2011.

[13] Y. Xu, H. Wang, Y. G. Li, and B. Pei, "Image encryption based on synchronization of fractional chaotic systems," *Communications in Nonlinear Science and Numerical Simulation*, vol. 19, no. 10, pp. 3735–3744, 2014.

[14] P. Zhou, R. Ding, and Y.-X. Cao, "Multi drive-one response synchronization for fractional-order chaotic systems," *Nonlinear Dynamics*, vol. 70, no. 2, pp. 1263–1271, 2012.

[15] D. Y. Chen, C. F. Liu, C. Wu, Y. J. Liu, X. Y. Ma, and Y. J. You, "A new fractional-order chaotic system and its synchronization with circuit simulation," *Circuits, Systems, and Signal Processing*, vol. 31, no. 5, pp. 1599–1613, 2012.

[16] H.-Y. Jia, Z.-Q. Chen, and W. Xue, "Analysis and circuit implementation for the fractional-order Lorenz system," *Acta Physica Sinica*, vol. 62, no. 14, Article ID 140503, 2013.

[17] X. Li and R. C. Wu, "Hopf bifurcation analysis of a new commensurate fractional-order hyperchaotic system," *Nonlinear Dynamics*, vol. 78, no. 1, pp. 279–288, 2014.

[18] P. Muthukumar, P. Balasubramaniam, and K. Ratnavelu, "Synchronization and an application of a novel fractional order King Cobra chaotic system," *Chaos*, vol. 24, no. 3, Article ID 033105, 2014.

[19] L. Liu, W. Ding, C. X. Liu, H. G. Ji, and C. Q. Cao, "Hyperchaos synchronization of fractional-order arbitrary dimensional dynamical systems via modified sliding mode control," *Nonlinear Dynamics*, vol. 76, no. 4, pp. 2059–2071, 2014.

[20] M. P. Aghababa, "Design of a chatter-free terminal sliding mode controller for nonlinear fractional-order dynamical systems," *International Journal of Control*, vol. 86, no. 10, pp. 1744–1756, 2013.

[21] G.-S. Wang, J.-W. Xiao, Y.-W. Wang, and J.-W. Yi, "Adaptive pinning cluster synchronization of fractional-order complex dynamical networks," *Applied Mathematics and Computation*, vol. 231, pp. 347–356, 2014.

[22] V. Vembarasan and P. Balasubramaniam, "Chaotic synchronization of Rikitake system based on T-S fuzzy control techniques," *Nonlinear Dynamics*, vol. 74, no. 1-2, pp. 31–44, 2013.

[23] C. K. Ahn, "Takagi-Sugeno fuzzy receding horizon H_∞ chaotic synchronization and its application to the Lorenz system," *Nonlinear Analysis. Hybrid Systems*, vol. 9, pp. 1–8, 2013.

[24] M. Chadli and T. M. Guerra, "LMI solution for robust static output feedback control of discrete Takagi-Sugeno fuzzy models," *IEEE Transactions on Fuzzy Systems*, vol. 20, no. 6, pp. 1160–1165, 2012.

[25] M. R. Faieghi and H. C. Delavari, "Chaos in fractional-order Genesio-Tesi system and its synchronization," *Communications in Nonlinear Science and Numerical Simulation*, vol. 17, no. 2, pp. 731–741, 2012.

[26] F. Q. Wang and C. X. Liu, "Study on the critical chaotic system with fractional order and circuit experiment," *Acta Physica Sinica*, vol. 55, no. 8, pp. 3922–3927, 2006.

[27] L.-X. Yang and J. Jiang, "Adaptive synchronization of drive-response fractional-order complex dynamical networks with uncertain parameters," *Communications in Nonlinear Science and Numerical Simulation*, vol. 19, no. 5, pp. 1496–1506, 2014.